JOURNAL OF AGRICULTURAL AND FOOD CHEMISTRY

Article

pubs.acs.org/JAFC

Molecular Approach to the Synergistic Effect on Astringency Elicited by Mixtures of Flavanols

Alba María Ramos-Pineda,[†] Ignacio García-Estévez,[†,§] Natércia F. Brás,[⊗] Eva M. Martín del Valle,[‡] Montserrat Dueñas,[†] and María Teresa Escribano Bailón*[,†]

[†]Grupo de Investigación en Polifenoles (GIP), Facultad de Farmacia, University of Salamanca, Salamanca, Spain

[§]LAQV, REQUIMTE, Faculdade de Ciências, Universidade do Porto, Porto, Portugal

[⊗]UCIBIO, REQUIMTE, Faculdade de Ciências, Universidade do Porto, Porto, Portugal

[‡]Department of Chemical Engineering, University of Salamanca, Salamanca, Spain

Supporting Information

ABSTRACT: The interactions between salivary proteins and wine flavanols (catechin, epicatechin, and mixtures thereof) have been studied by HPLC-DAD, isothermal titration microcalorimetry, and molecular dynamics simulations. Chromatographic results suggest that the presence of these flavanol mixtures could facilitate the formation of precipitates to the detriment of soluble aggregates. Comparison between the thermodynamic parameters obtained showed remarkably higher negative values of ΔG in the system containing the mixture of both flavanols in comparison to the systems containing individual flavanols, indicating a more favorable scenario in the mixing system. Also, the apparent binding constants were higher in this system. Furthermore, molecular dynamics simulations suggested a faster and greater cooperative binding of catechin and epicatechin to $IB7_{14}$ peptides when both types of flavanols are present simultaneously in solution.

KEYWORDS: *astringency, flavan-3-ols, proline-rich proteins, salivary proteins, isothermal titration calorimetry, molecular dynamics simulations*

INTRODUCTION

Flavan-3-ols are a large and complex group of compounds commonly found in plants, foods, and beverages. In red wine they exist in the form of oligomers and polymers composed of four main flavan-3-ols: catechin, epicatechin, gallocatechin, and epigallocatechin.[1] Several of these compounds have the ability to precipitate proteins, which in turn is the main mechanism for the development of the astringency sensation.[2−6] Astringency has been defined as "the complex of sensations due to shrinking, drawing or puckering of the epithelium as a result of exposure to substances such as alums or tannins" by the American Society for Testing Materials.[7] Although the mechanism of astringency is not well understood yet,[8] the most accepted one consists of the interaction between tannins and some specific salivary proteins,[9] namely, proline-rich salivary proteins, a type of conformationally open proteins (random coils). These interactions would form soluble aggregates that become insoluble after the binding of additional tannins to the complex and, consequently, precipitate.[10−12] Other studies have proposed different mechanisms such as disruption of the salivary film in the oral cavity or a direct interaction of the aggregates with receptors.[10,13]

Saliva is a complex hypotonic aqueous solution with high variability and dynamic behavior, which make it arduous to study.[14] Salivary proteins have been grouped according to their structure and characteristics, namely, α-amylases, mucins, carbonic anhydrases, statherins, P-B peptide, histatins, cystatins, and proline-rich proteins (PRPs), which are in turn divided into acidic (aPRPs), basic (bPRPs), and glycosylated (gPRPs).[15] Salivary proline-rich proteins PRPs represent >60% by weight of the total salivary proteome,[14,15] and are particularly effective in complexing tannins.[16] This interaction could be favored due to the presence of repeated proline-rich regions that provide sites for tannin binding, and it has been reported that hydrophobic and hydrogen bonds are the main driving force.[17]

On the other hand, several authors have stated that the structure and stereochemistry of tannins influence their ability to bind proteins, and hence the astringent sensation is elicited. For instance, some studies have shown that (−)-epicatechin is perceived as more bitter and more astringent than (+)-catechin[2,8] and that esterification with gallic acid increases the interaction with proline-rich proteins such as poly(L-proline).[18] Recently, the existence of mechanisms of synergy has also been pointed out, consisting of an increase in the intensity of astringency when mixtures of phenolic compounds are tested, in comparison with the phenolic compounds tested alone, maintaining constant the amount of stimulus.[8]

Sensory analysis is nowadays the best method to describe and qualify the astringency.[9] Nevertheless, it has several inconveniences such as the impossibility of explaining at the molecular level the mechanisms underlying that complex sensation. As an alternative, methodologies such as NMR

Special Issue: XXVIIIth International Conference on Polyphenols 2016

Received: April 6, 2017
Revised: April 10, 2017
Accepted: April 19, 2017
Published: April 19, 2017

DOI: 10.1021/acs.jafc.7b01600
J. Agric. Food Chem. XXXX, XXX, XXX−XXX

spectroscopy, electrophoresis, protein precipitation, turbidity, nephelometry, fluorescence, or isothermal titration microcalorimetry (ITC) have been used to analyze tannin−protein complexation.[19−21] This last technique is considered the most direct method to measure the heat change on formation of a complex at constant temperature.[22,23] However, the interpretation of the results from these studies can be laborious because polyphenol−protein interactions do not follow the classical "lock and key" model.[11,22]

The aim of this work was to go deeper into the knowledge of the interaction between flavanols and proteins as a relevant mechanism for explaining the astringency. In the literature, there are interesting and revealing studies focused on assessing the interaction between different kinds of saliva-model proteins (bovine serum albumin, poly(L-proline), recombinant PRP IB-5) and individual flavanols.[18,23−26] Nevertheless, there are very few studies performed with saliva. Because in foods and beverages different structures are likely to be present as putative ligands of salivary proteins, we have evaluated by HPLC-DAD, ITC, and molecular dynamics (MD) simulation the behavior of ternary mixtures of salivary proteins/catechin/epicatechin in comparison to the binary systems of salivary proteins/catechin and salivary proteins/epicatechin, maintaining constant the amount of flavanol. With this approach we intend to obtain evidence, using instrumental objective techniques, to support the synergisms of the astringency between flavanols that have been proposed in previous studies using sensory analysis.[8]

MATERIALS AND METHODS

Reagents. All reagents used were of analytical grade, and all solvents were of HPLC grade. (+)-Catechin (CAT) and (−)-epicatechin (EC) were purchased from Sigma-Aldrich (St. Louis, MO, USA). Trifluoroacetic acid (TFA) was purchased from Riedel-de Haën (Hanover, Germany). Ultrapure water was obtained from a Milli-Q Gradient water purification system (Millipore, Billerica, MA, USA).

Saliva Collection and Treatment. Whole human saliva was collected from six healthy, nonsmoker volunteers (three men and three women aged between 24 and 50 years old). They were previously instructed to avoid foods and beverages for at least 1 h before collection. Collection time was set at 10:30 a.m. to reduce variability due to circadian rhythms of saliva secretion.[27] The saliva pool was immediately treated with 10% TFA (final concentration of 0.1%) to inhibit protease activity[28] and to precipitate high molecular weight proteins such as mucins.[28,29] After that, the sample was centrifuged for 10 min at 12000*g*, and the supernatant was dialyzed using a Spectra/Por 3 cellulose membrane (SpectrumLabs) with an exclusion size of 3.5 kDa. The dialysis process was carried out using ultrapure water, at 10 °C for 48 h, renewing the water every 8 h. Treated saliva (SP) was analyzed by HPLC-DAD. Seven SP fractions were collected at the DAD chromatographic detector outlet. Identification was carried out after tryptic digestion and nLC-MS-MS analysis. Digestion was performed as described by Link et al.[30] as modified by Quijada-Morín et al.[31] Briefly, lyophilized proteins were resolubilized in 8 M urea/50 mM NH_4−HCO_3, reduced, and alkylated using 100 mM dithiothreitol (DTT) and 200 mM iodoacetamide (IAA), and then 100 mM DTT was added to quench unreacted IAA. Endoproteinase Lys-C was added to a final substrate/enzyme ratio of 100:1, and the reaction was incubated (37 °C, 4 h). The Lys-C digestion was diluted 4-fold with 50 mM NH_4HCO_3, and modified trypsin was added to a final substrate/enzyme ratio of 50:1. The trypsin digestion was incubated at 37 °C for 16 h. Purification of tryptic peptides was performed with C18 Stagetips, and an aliquot ($^1/_{20}$) of the sample containing the generated tryptic peptides was diluted in 0.5% formic acid/ACN (97/3), prior to analysis by nLC-MS/MS. A nano-UPLC system (nanoAcquity, Waters Corp., Milford, MA, USA) coupled to an LTQ-Orbitrap Velos mass spectrometer (ThermoFisher Scientific, San Jose, CA, USA) via a nanoelectrospray ion source (NanoSpray flex, Proxeon, Thermo) (nanoAcquity, Waters Corp., Milford, MA,USA) was used for the identification.[31]

Interaction Assays by HPLC-DAD. One hundred and twenty-five microliters of SP was mixed with 125 μL of the flavan-3-ol solution (1 g L^{-1} in 0.1 M acetate buffer, pH 5) and kept at room temperature during 30 min. Three different systems were studied: SP-CAT, SP-EC, and SP-CAT-EC. This last was prepared with a mixture (1:1) of CAT and EC. Prior to the chromatographic analysis, samples were filtered through 0.45 μm. HPLC-DAD analysis was carried out as described in Quijada-Morín et al.[31] HPLC-DAD analysis was performed in an Agilent 1200 series HPLC system (Agilent Technologies, Palo Alto, CA, USA) consisting of an autosampler, a quaternary pump, a vacuum degasser, a thermostated column compartment, and a diode array detector (DAD) that were controlled by ChemStation software (version B.04.01; Agilent Technologies). A Zorbax 300SB-C8, 5 μm (2.1 × 150 mm), column was used. The solvents used were (A) aqueous TFA 0.1% and (B) TFA 0.1% in acetonitrile, establishing the following gradient: 8−12% B in 10 min, 12−32% B in 50 min, followed by washing and re-equilibration of the column to initial conditions. The flow rate was set at 0.3 mL min^{-1}, and the injection volume was 90 μL. Detection was carried out at 214 nm as the preferred wavelength. All experiments were performed in triplicate and were compared to a SP control without flavanol.

Isothermal Titration Calorimetry (ITC) Assays. A Nano microcalorimeter (TA Instruments, New Castle, DE, USA) was used to measure enthalpy changes associated with SP−flavanol interactions at 283 K. The titrant was a flavanol solution containing CAT or EC or a mixture (CAT+EC) (concentration of flavanol in the three systems = 10 mM). The flavanol solution was loaded into the injection syringe, and the SP solution (0.025 mM) was placed into the 1 mL sample cell of the calorimeter. The average molecular weight of saliva (10,000 Da) was estimated from the percentage of each salivary fraction obtained in the HPLC-DAD analysis and the molecular weight of the corresponding proteins obtained in the literature.[29,32−36] All of the solutions were prepared in sodium acetate buffer, pH 5, with the ionic strength adjusted with 100 mM sodium chloride. Flavanol solution (10 mM in sodium acetate buffer pH 5.0) was titrated into the sample cell as a sequence of 25 injections of 10 μL aliquots, and the time delay (to allow equilibration) between successive injections was 400 s. The contents of the sample cell were stirred throughout the experiment at 400 rpm. The raw data obtained from ITC were transformed using AFFINIMETER software (Software for Science Developments) to build a plot of heat change versus flavanol/protein molar ratio. The resulting curve was fitted with the AFFINIMETER software using the independent sites model with two set of sites, because it was the model that best fitted the observed behavior. Fitting allowed obtaining the binding apparent constant (K_{app}), the number of binding sites per molecule (n), and the thermodynamic parameters of the interaction. Free energy (ΔG) was determined from the binding constant ($\Delta G = -RT \ln K$, where R is the gas constant and T is the absolute temperature in Kelvin). Entropy was obtained from the second law of thermodynamics ($\Delta G = \Delta H - T\Delta S$). Control samples using flavanol aqueous solutions were performed, and negligible variations of energy were obtained.

Optimization and Molecular Dynamics Simulations. Three different molecular systems composed of the $IB7_{14}$ PRP fragments and several flavanols (CAT and/or EC) molecules were built. The amino acid sequence of $IB7_{14}$ is SPPGKPQGPPPQGG. The CAT and EC molecules were optimized with the HF/6-31G(d) level of theory by using the Gaussian 09 suite of programs,[37] followed by their parametrization using the antechamber tool and the RESP algorithm[38] to get the atomic charges.

The molecular systems comprise four $IB7_{14}$ peptides and (1) eight CAT, (2) eight EC, and (3) four CAT and four EC. The CAT molecules were randomly placed around the peptides, reproducing the experimental conditions. The position of these flavonoids was used to create the other systems to better compare the results. Because the third system may have different CAT+EC order combinations, we created three different systems to get an average of the various

DOI: 10.1021/acs.jafc.7b01600
J. Agric. Food Chem. XXXX, XXX, XXX−XXX

possibilities. Therefore, the average values of the three simulations for the $(IB7_{14})$4:(CAT)4:(EC)4 system are shown and discussed in the next sections. Four chloride counterions were added to neutralize each system. To reproduce an explicit solvation, a rectangular box of TIP3P waters with a minimum distance of 15 Å between the box edges and any atom within each system was included. Geometry optimization and MD simulations were carried out using the GAFF[39] and ff99SB[40] force fields for flavanols and peptides, respectively. The minimization occurred in two stages: (1) only the position of water molecules and the counterions were optimized and (2) the whole system was minimized. All systems were equilibrated by 100 ps of MD simulations with an NVT ensemble (constant number of particles, volume, and temperature) and considering periodic boundary conditions. Subsequently, 50 ns of MD simulations with an isothermal−isobaric NPT (constant number of particles, pressure, and temperature) ensemble using the Langevin thermostat (collision frequency of 1.0 ps^{-1})[41] and the Berendson barostat were performed. The SHAKE algorithm was used to constrain the hydrogen bond lengths, and the equations of motion were integrated with a 2 fs time step using the Verlet leapfrog algorithm.[42] The particle-mesh Ewald (PME) method[43] was used to treat long-range interactions, and the nonbonded interactions were truncated with a 10 Å cutoff. The AMBER 12.0[44] simulations package was used to run all minimizations and simulations. The PTRAJ module of AMBER 12.0 and the Visual Molecular Dynamics 1.9.1 software[45] were used to analyze and visualize, respectively, the MD trajectories.

Statistical Analysis. To determine the statistical significance of the difference between the chromatographic areas, data were evaluated by variance (ANOVA) and post hoc Tukey HSD test, using the software package for Windows IBM SPSS 21 (SPSS, Inc. Chicago, IL, USA). Differences were considered to be statistically significant when $P < 0.05$.

RESULTS AND DISCUSSION

In a previous sensory study[8] we have described the existence of synergism of astringency between flavanols when they were tested as a mixture in comparison with the same flavanols tested individually. To obtain objective insights into the synergistic astringent effect observed, we have studied by HPLC-DAD, ITC, and MD simulations the interaction between salivary proteins and catechin, epicatechin, and a mixture of both, maintaining constant the amount of flavanols.

Interaction Assays by HPLC-DAD. The chromatographic conditions for the analysis of SP were previously optimized in our laboratory. Seven fractions were clearly separated and isolated, and their proteins and peptides identified after tryptic digestion. To determine the effect of the addition of the studied flavan-3-ols in the chromatographic salivary profile registered at 214 nm, the chromatographic areas of the different fractions were obtained after injection of the three studied systems (CAT, EC, and CAT+EC) and compared to those corresponding to the SP control.

Statistically significant differences between the studied systems were observed for fractions 1 (bPRP), 3 (gPRP), 4 (histatine), and 7 (statherin) (Table 1). Figure S1 in the Supporting Information shows the chromatographic salivary profile and the chromatographic profiles of the fractions that underwent significant changes after the addition of CAT, EC, and CAT+EC. Fraction 1 shows an important significant increase in the chromatographic area when SP is incubated in the presence of EC (35.0%), whereas a significant decrease in the chromatographic area of this fraction was obtained in the CAT assays (−22.6%) (Table 1). The increase in the chromatographic area for EC could be understood as the formation of soluble aggregates of flavanol−protein eluting in this zone,[31] which were not observed in the presence of catechin. Because the mixture CAT+EC results in a small

Table 1. Percentage Decrease (−) or Increase (+) in the Chromatographic Area of Each Salivary Protein Fraction after Interaction Assays with CAT, EC, and CAT+EC (1:1)[a]

fraction	CAT	EC	CAT+EC (1:1)
1 (bPRP)	−22.6 ± 0.1*	+35.0 ± 2.6*	+4.3 ± 3.7*
2 (PB peptide)	−6.6 ± 5.8	+7.0 ± 6.0	−5.5 ± 0.4
3 (gPRP)	−2.7 ± 3.5*	−7.4 ± 1.2	−12.8 ± 0.7*
4 (His-3)	+1.5 ± 1.0	+4.4 ± 2.4*	−4.9 ± 0.9*
5 (aPRP)	−2.1 ± 2.1	−2.8 ± 3.9	+0.7 ± 0.8
6 cystatins	+2.3 ± 2.5	+0.1 ± 1.6	+4.0 ± 1.2
7 statherin	−46.5 ± 4.8*	−19.6 ± 3.3*	−31.7 ± 4.3*

[a]An asterisk indicates statistical differences ($\alpha = 0.05$) among samples.

increase in the area (4.3%), it could be interpreted as a hindrance in the formation of the soluble aggregates in which epicatechin is involved. In fraction 3, the mixture CAT+EC shows a higher decrease in the chromatographic area (−12.8%) than was observed for CAT (−2.7%, statistical significance) and EC (−7.4%, no statistical significance). This might indicate the existence of a kind of cooperation between both flavanols that facilitates the interaction with salivary proteins, resulting in a higher formation of insoluble aggregates. A similar behavior seems to occur in fraction 4: CAT+EC shows a decrease in the chromatographic area, whereas it was not observed for CAT or EC experiments. As for fraction 7, a clear significant decrease in CAT, EC, and CAT+EC assays was observed, although this does not suggest that the mixture CAT+EC could affect the interaction with the protein, because CAT+EC seems to have a behavior intermediate between those of CAT and EC.

The results in Table 1 may indicate the existence of a synergistic behavior in CAT+EC mixtures. Therefore, to gain better insight into the protein−flavanols interactions that produce the observed effects, further experiments were performed by ITC and MD simulations.

Isothermal Titration Calorimetry. ITC is an interesting technique based on the measurement of the heat generated or absorbed upon the interaction between ligands and has been widely used for the characterization of the interaction mechanisms between ligands and macromolecules, including proteins, DNA, carbohydrates,[46] and even microorganisms.[47]

In relatively complex systems such as the ones tested herein, changes in the enthalpy measured with ITC can arise from a combination of several processes as flavanol−protein(s) binding, self-aggregation between proteins or ligands or between the complexes formed, and also possible changes in the conformation of the protein(s) or of the flavanol. In such systems, an estimation of the apparent constant and the thermodynamic parameters of the global process might be obtained. However, the interpretation of the results from these studies can be laborious because polyphenol−protein interactions do not follow the classical "lock and key" model.[11,22]

In our case, we expect that the comparison of the parameters obtained in the system "pure flavanol−salivary proteins" toward the system "mixture of flavanols−salivary proteins" could give insights for explaining the synergistic effect of astringency previously described for mixtures of flavanols[8] and also to make a more realistic approach to the astringency phenomenon.

Figure 1 shows the isotherm fitting for the system CAT−salivary proteins (Figure 1A) and for the system EC−salivary proteins (Figure 1B). In both cases, it can be observed that, globally, the released energy indicates spontaneous processes. This has also been inferred in the literature for the interaction

DOI: 10.1021/acs.jafc.7b01600
J. Agric. Food Chem. XXXX, XXX, XXX−XXX

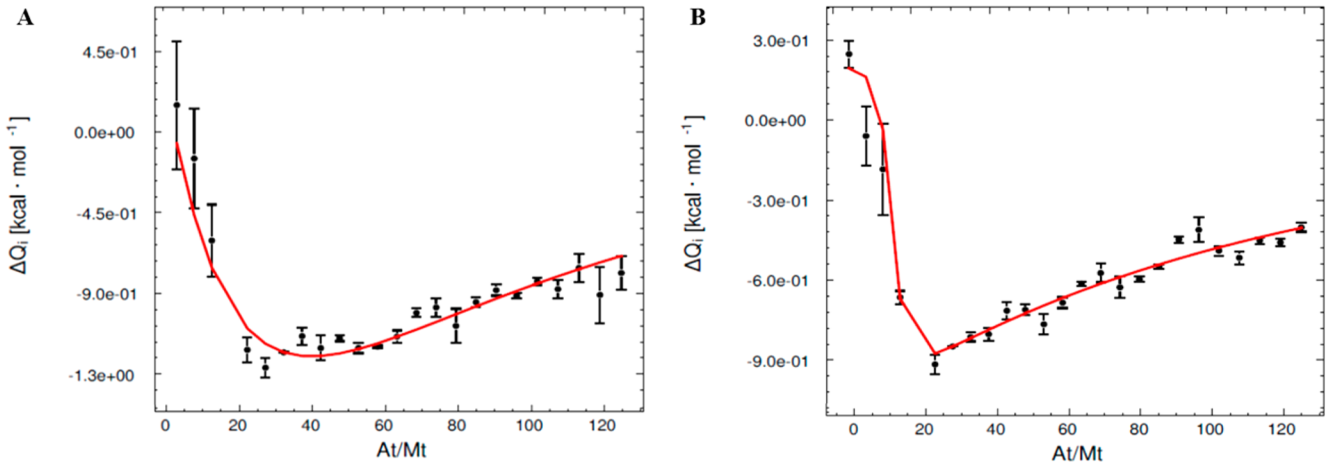

Figure 1. Isotherm fitting for the system catechin−salivary proteins (A) and for the system epicatechin−salivary proteins (B). At/Mt: ratio tannin/protein.

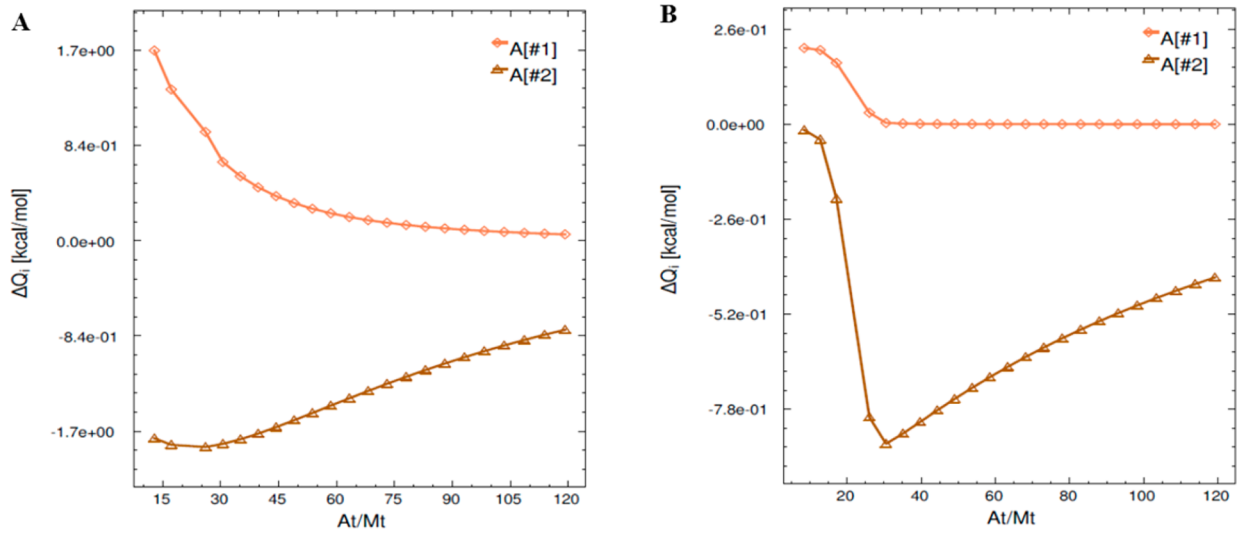

Figure 2. Contributions to the binding isotherm for catechin (A) and epicatechin (B). The fitting considers two sets: set A1 and set A2. At/Mt: ratio tannin/protein.

Table 2. Thermodynamic Parameters for the Interactions CAT−Salivary Proteins, EC−Salivary Proteins, and CAT+EC−Salivary Proteins

			CAT+EC	
	CAT	EC	A	B
		Set 1		
r_M	0.771 ± 0.003	0.694 ± 0.002	0.8000 ± 0.0008	
r_A	0.901 ± 0.001	1.050 ± 0.001	1.0009 ± 0.0002	0.982 ± 0.002
n_1	10.24 ± 0.07	19.9 ± 0.4	24.98 ± 0.01	
K_1 (M^{-1})	(5.4 ± 0.2) × 10^3	(3.3 ± 0.7) × 10^5	(6.4 ± 0.1) × 10^7	(3.0732 ± 0.0001) × 10^7
ΔH_1 (cal mol^{-1})	7300 ± 100	200 ± 60	−52000 ± 100	30700 ± 30
ΔG_1 (cal mol^{-1})	−4800 ± 100	−7100 ± 900	−10100 ± 100	−9700 ± 100
$-T\Delta S_1$ (cal mol^{-1})	−12100 ± 200	−7300 ± 900	41900 ± 200	−40400 ± 70
		Set 2		
n_2	82.02 ± 0.06	90.0 ± 0.3	37.31 ± 0.03	
K_2 (M^{-1})	(5.99 ± 0.04) × 10^2	(1.80 ± 0.06) × 10^2	(2.046 ± 0.002) × 10^7	(5.316 ± 0.008) × 10^6
ΔH_2 (cal mol^{-1})	−5571 ± 8	−4400 ± 80	20210 ± 30	−30190 ± 50
ΔG_2(cal mol^{-1})	−3600 ± 80	−2900 ± 200	−9500 ± 300	−8700 ± 200
$-T\Delta S_2$(cal mol^{-1})	1970 ± 20	1500 ± 200	−29700 ± 300	21500 ± 300
χ^2	3.38	4.11	2.48	

DOI: 10.1021/acs.jafc.7b01600
J. Agric. Food Chem. XXXX, XXX, XXX−XXX

between individual flavanols and other types of proteins such as poly(L-proline)[18] and bovine serum albumin.[48] Besides, it is worth noting that the heat released increases at the beginning of the essay up to the fifth injection and then it experiences a decrease. A similar behavior has been stated in Poncet-Legrand et al.[18] and Frazier et al.,[49] who studied tannin−protein interaction, and it was interpreted as cooperative binding of the ligand to the protein,[18] probably due to an alteration of the protein molecular structure.[50]

The software used for the data treatment offers models contemplating multiple independent binding sites. The fitting function thus obtained contains a number of sets, in which the number of binding sites corresponds to a fitting parameter. The model that best fits the isothermal data considers two sets (set 1 and set 2 in Figure 2A for catechin and in Figure 2B for epicatechin) and independent sites. The thermodynamic parameters obtained, that is, apparent binding constant (K_{app}), number of binding sites in each set (n), free energy change (ΔG), change in enthalpy (ΔH), and change in entropy (ΔS) of each system are presented in Table 2. It can be observed that, for both flavanols, the first set (set 1) is entropy-driven, indicating dominance of hydrophobic interactions. Thus, the cooperative binding, previously mentioned, could be mainly governed by hydrophobic interactions and hence involve A and/or B rings of the flavanol structure and proline rings. Although theoretical sites for hydrophobic contacts are being occupied, the process could become less relevant, which may explain the saturation kinetics displayed (Figure 2). By contrast, the second set (set 2) is enthalpy-driven, indicating that hydrogen bonding is involved and, therefore, the more widely distributed C═O, H—N, and −OH groups. Accordingly, the number of theoretical binding sites (n) is higher in the enthalpy-driven set (set 2) than in the entropy-driven set for the both systems. These two sets (terms of the fitting equation) are in concordance with the main forces of interaction implicated in the interaction between flavanols and proteins, namely, hydrophobic interactions and hydrogen bonding.[2,51,52] This supports the suggestion recently proposed by Kilmister et al.[53] that the tannin binding to proteins involves multiple sites, with different association constants and ΔH values of binding.

Because the free energy change is negative for both flavanols, and for the two sets, the process is spontaneous. However, the more negative ΔG values obtained in the epicatechin system could indicate higher affinity of this flavanol than of catechin to the salivary proteins. Furthermore, for the first set, the K_{app} obtained for epicatechin system was noticeably higher than the K_{app} obtained for catechin system (3.3×10^5 and 5.4×10^3, respectively). This would be in good agreement with the fact that epicatechin is more astringent and persistent than catechin when they are tasted by a trained sensory panel.[8,54,55]

With regard to the system formed by the mixture of flavanols and salivary proteins (CAT+EC−salivary proteins), we have also considered, in the fitting software, two sets of binding sites and furthermore the existence of two mixed molecules (A and B) in the titrant solution. Figure 3 shows the isotherm fitting for this system and Figure 4 the contribution of the four terms to the equation. The isotherm shows a different shape than those obtained for the systems with individual compounds. Nevertheless, we can observe the same two types of contribution to the binding isotherm: on the one hand, the endothermic hydrophobic component (sets B1 and A2 in Figure 4) and, on the other hand, the exothermic hydrogen

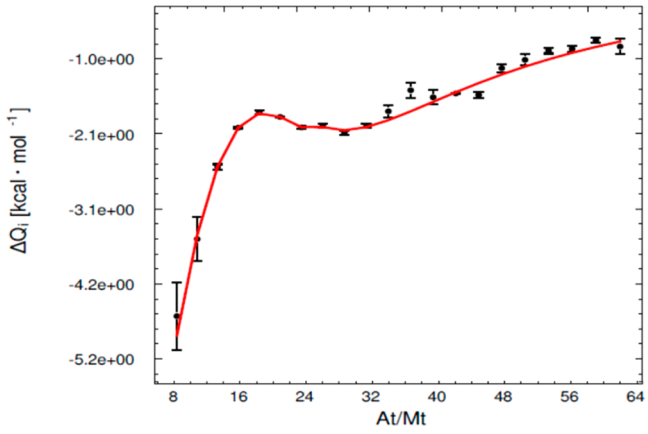

Figure 3. Isotherm fitting for the system catechin+epicatechin−salivary proteins. At/Mt: ratio tannin/protein.

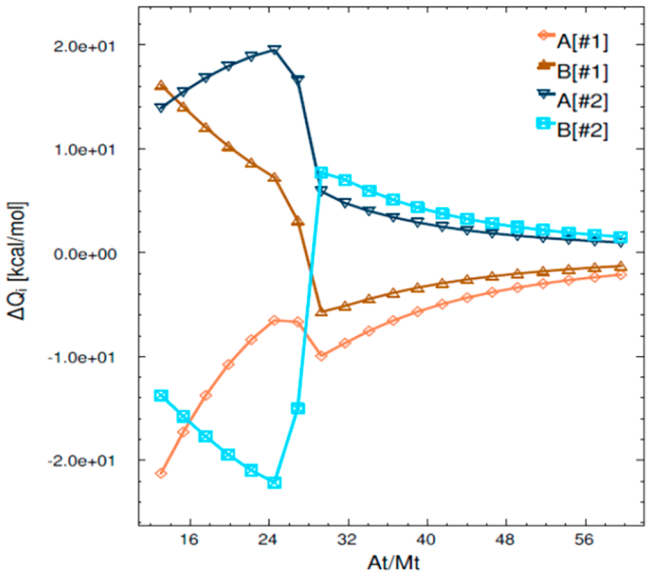

Figure 4. Contributions to the binding isotherm for the mixture catechin+epicatechin. The fitting considers four terms into the equation: set A1, set A2, set B1, and set B2. At/Mt: ratio tannin/protein.

bond component (sets B2 and A1 in Figure 4). It has become apparent that the contribution of the hydrophobic component for one of the molecules (B) is higher than for the other one (A), because the $-T\Delta S$ value is −40,400 cal mol^{-1} for B1 and −29,700 cal mol^{-1} for A2. The opposite occurs for the hydrogen bond component: the $-T\Delta S$ value is 21,500 cal mol^{-1} for B2 and 41,900 cal mol^{-1} for A1. Although we cannot know the identity of molecule A or molecule B, MD simulations carried out and discussed below seem to support that interactions by hydrogen bonds could be more relevant for EC−protein interaction than for CAT−protein interaction.

The comparison between the thermodynamic parameters obtained from the three systems studied showed remarkably higher negative values of ΔG in the system containing the mixture of both flavanols (CAT+EC−salivary proteins) in comparison to the systems containing individual flavanols (i.e., CAT−salivary proteins system and EC−salivary proteins system), indicating a more favorable scenario in the mixing system. Also, the apparent binding constants are higher in this system. This is consistent with the more intense sensation of

DOI: 10.1021/acs.jafc.7b01600
J. Agric. Food Chem. XXXX, XXX, XXX−XXX

astringency obtained in sensory analysis when the mixture of flavanols was tested in comparison with the same flavanols tested alone, maintaining constant the concentration (amount of stimulus).[8]

Molecular Dynamics Simulations. MD simulations are one of the principal tools in the theoretical study of biological molecules. MD simulation is a computational method that usually uses model molecules and that serves as a complement to conventional experiments.[56] To perform these experiments, we have selected the $IB7_{14}$ peptide, which belongs to the PRP family and that has been widely used as a representative peptide of human saliva in model studies.[2,22] Several 50 ns MD simulations were carried out to understand, at an atomistic level, the recognition and interaction of two different types of flavanols to $IB7_{14}$ peptidic fragments in an aqueous environment. Figure 5 displays a representative structure of each system in which the $IB7_{14}$–flavanols interactions are maximized. The formation of stable complexes involving one, two, or three flavanols and several residues of the peptides was observed. Figure S2 in the Supporting Information shows enlarged pictures of the simultaneous binding of different flavanols to the peptide. Some of these molecules remained bound during most of the simulation, whereas others would interact quickly and with different partners. Both catechin and epicatechin interact preferentially with the proline and glycine regions of the peptide. The CAT molecules interact with Pro3, Gly8-Pro9, and Gly14, whereas the EC compounds interact with the backbone groups of Gly4-Pro9. The formation of EC:EC complexes (Figure 5), in which hydrophobic interactions occur during the alignment of their planar phenolic ring surfaces, was also seen.

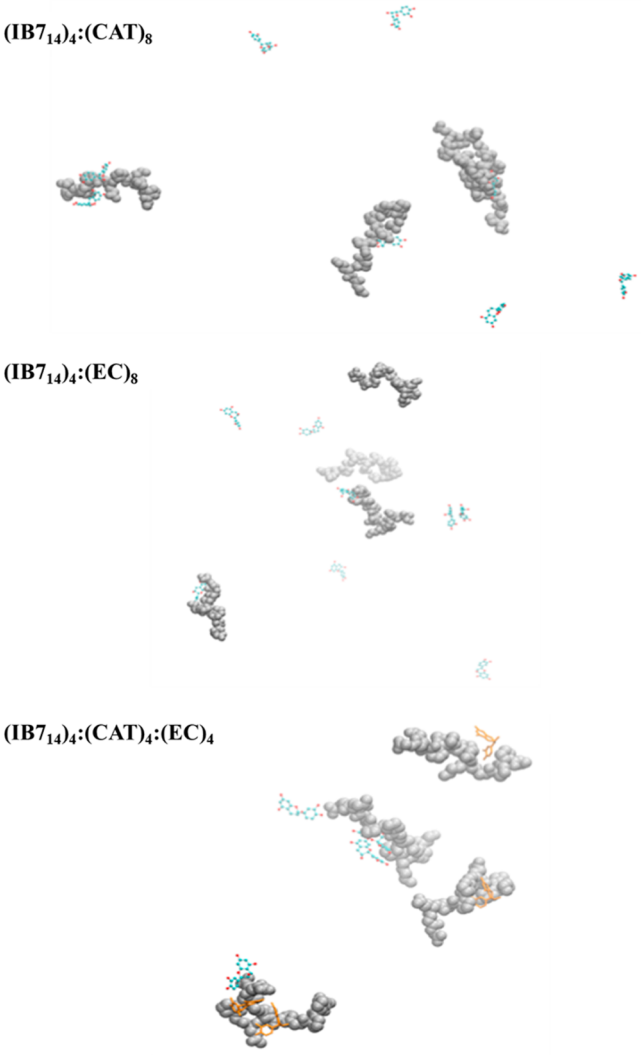

Figure 5. Illustration of representative geometries of $(IB7_{14})_4$:$(CAT)_8$, $(IB7_{14})_4$:$(EC)_8$, and $(IB7_{14})_4$:$(CAT)_4$:$(EC)_4$ systems extracted from each MD simulation. The peptides are depicted with vdW and are colored silver. The CAT and EC molecules are depicted with ball and stick representationd and are colored by element type (except the CAT compounds in the third system that are colored orange).

The average and maximum times of the formation of $(IB7_{14})_1$:$(flavanol)_n$ complexes throughout simulations were used as indicators to evaluate the binding affinities of CAT and EC to this salivary peptide. Table 3 summarizes these values obtained for the 50 ns simulations. The average and the sum of total binding time of one flavanol are higher in the simulations with individual CAT or EC compounds than in the simulations with both molecules (19.9, 20.1, and 14.4 ns average values, respectively). However, the simultaneous binding of more than two molecules was observed only in the simulation with both flavanols. Figure 6 shows a stable complex over time formed by two peptide molecules, three epicatechin and one catechin. Epicatechin molecules interact between them and are disposed between the two peptides to form the complex. Please note that the bottom panels of Figures 5 and 6 occur in different times of simulation (31 and 43 ns, respectively). It could be hypothesized that the structural difference between catechin and epicatechin (more planar) could provoke a global entropic effect. The more planar structure of epicatechin (due to the position of the OH in the C ring) enables a better interaction

Table 3. Binding of CAT and EC Molecules to Four $IB7_{14}$ PPR Fragments Analyzed by Time of Binding and Number of Flavanols Bound Simultaneously to Each Peptide throughout the 50 ns Simulations[a]

system		one flavanol	two flavanols	three flavanols	time of binding of the first flavanol (ns)
CAT	$IB7_{14\_1}$	10.2	0.0		38.8
	$IB7_{14\_2}$	28.1	0.0		21.2
	$IB7_{14\_3}$	21.2	11.4		17.1
	$IB7_{14\_4}$	20.3	0.0		21.1
	average	19.9	2.9		24.6
	sum	79.7	11.4		
EC	$IB7_{14\_1}$	6.2	0.0		16.7
	$IB7_{14\_2}$	21.7	3.5		8.9
	$IB7_{14\_3}$	28.8	0.2		17.3
	$IB7_{14\_4}$	23.6	2.8		23.5
	average	20.1	1.6		16.6
	sum	80.2	6.5		
CAT +EC	$IB7_{14\_1}$	27.2	3.4	0.9	15.1
	$IB7_{14\_2}$	7.6	11.1	8.4	8.1
	$IB7_{14\_3}$	9.5	0.0	0.0	8.6
	$IB7_{14\_4}$	13.2	5.1	0.6	16.2
	average	14.4	4.9	2.5	12.0
	sum	57.5	19.5	9.9	

[a]The average and total binding times of peptide–polyphenol interactions are also shown.

DOI: 10.1021/acs.jafc.7b01600
J. Agric. Food Chem. XXXX, XXX, XXX–XXX

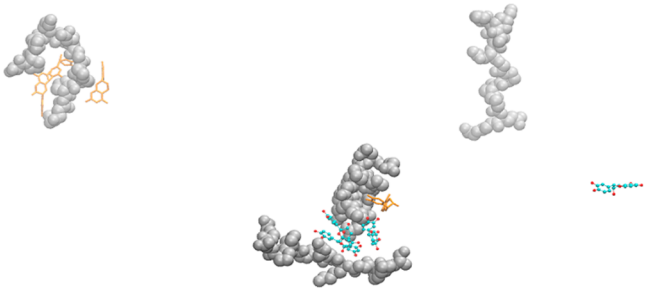

Figure 6. Illustration of $(IB7_{14})_4$:$(CAT)_4$:$(EC)_4$ system in which a complex formed by two peptide molecules, three epicatechins, and one catechin can be observed. The peptides are depicted with vdW and are colored silver. The CAT and EC molecules are colored blue (epicatechin) and orange (catechin).

between the phenolic ring surfaces, which in turn facilitates a faster and more effective interaction with peptides. In fact, in 75% of cases epicatechin interacts with the peptide before catechin. Furthermore, due to its more planar structure, epicatechin likely more easily forms hydrogen bonds between its hydroxyl groups and the polar groups of the peptide than catechin does. Once epicatechin interacts with the peptide, the formation of new cavities in the structure could facilitate the inclusion of catechin, with more distorted structure. Thus, the presence of both CAT and EC compounds in solution seems to produce a synergistic effect that causes them to bind more easily and efficiently to $IB7_{14}$ peptides. This is in good agreement with the ITC data.

Furthermore, it was also noted that the first interaction between a flavanol and an $IB7_{14}$ peptide occurs more rapidly in systems with both types of polyphenols present (24.6, 16.6, and 12.0 ns average values for CAT, EC, and CAT+EC systems, respectively). To evaluate the synergistic effect through time, the average and maximum times of the formation of $(IB7_{14})_1$:$(flavanol)_n$ complexes during the first half of each simulation were also determined. Table S1 in the Supporting Information displays these values. By comparison of these values with the ones from Table 3, it was observed that the synergistic effect is much more noticeable, because the binding of one flavanol occurs for significantly longer periods in the simulation with both types of flavanols in the solution (3.9, 3.0, and 7.6 ns average values for CAT, EC, and CAT+EC systems, respectively). These data suggest that the synergistic effect is higher in the first moments of contact between the flavanols and the $IB7_{14}$ peptides.

Interestingly, we observed the binding of a fewer polyphenols to $IB7_{14}$ peptides and a lesser association between the four peptides than observed in another study in which the interaction of some phenolic acids and $IB7_{12}$ peptides was evaluated.[57] Although the $IB7_{14}$ has two more additional glycine residues than the $IB7_{12}$, we consider that this fact probably occurs due to the bigger size of CAT and EC molecules when compared to the gallic, protocatechuic, caffeic, and *p*-coumaric acid molecules. In general, higher conformational rearrangements of peptides and time are required to accommodate and bind the larger flavanol molecules.

The binding of CAT and EC flavanols to $IB7_{14}$ peptides occurs by H-bonds involving the hydroxyl groups from the polyphenols and polar residues, as well as hydrophobic contacts between the polyphenolic planar ring surfaces and nonpolar residues of the PRP fragments, which is in agreement with the ITC data and with other studies involving proteins and polyphenols.[51,52]

These MD simulation results suggest a greater cooperative binding of CAT and EC to $IB7_{14}$ peptides when both types of flavanols are present simultaneously in solution. This synergistic binding effect was significantly evidenced in the first moments of contact and tends to decrease over the time of simulation.

As concluding remarks, studies performed by HPLC-DAD, ITC, and MD simulations point out the existence of a cooperative behavior between catechin and epicatechin when binding proteins that could explain the synergies of astringency evidenced when the sensory panel evaluated these compounds in a previous study.[8] It can be expected that the synergistic interactions also take place between other kinds of phenolic compounds and could, besides, be the origin of the multiple qualitative forms of astringency. Furthermore, it could additionally explain why astringency is more influenced by the qualitative phenolic composition than by the total concentration.[58] On the other hand, the synergic behavior of flavanol mixtures could be extrapolated as a general behavior of these compounds when they interact not only with salivary proteins but also with other biological and/or dietary proteins.

■ ASSOCIATED CONTENT

Supporting Information

The Supporting Information is available free of charge on the ACS Publications website at DOI: 10.1021/acs.jafc.7b01600.

Average and maximum times of the formation of $(IB7_{14})1$:$(flavanol)n$ complexes throughout the first 25 ns of MD simulations (Table S1). Chromatographic profile of saliva and of fractions 1, 3, 4, and 7 that underwent significant changes after addition of flavanols (Figure S1) and enlarged illustration of representative geometries of the binding of different flavanols to one $IB7_{14}$ peptide extracted from MD simulations (Figure S2) (PDF)

■ AUTHOR INFORMATION

Corresponding Author

*(M.T.E.-B.) Phone: +34 923 294 537. E-mail: escriban@usal.es.

ORCID

Ignacio García-Estévez: 0000-0001-8794-8328
Eva M. Martín del Valle: 0000-0002-9934-2769

Funding

We thank the Spanish MINECO (Project ref AGL2014-58486-C02-R-1 cofunded by FEDER) and to the EU for financial support under partnership agreement PT2020 (UID/QUI/50006/2013-POCI/01/0145/FEDER/007265). A.M.R.-P. also thanks MINECO for an FPI scholarship, and N.F.B. thankfully acknowledges her IF starting grant (IF/01355/2014) from Fundação para a Ciência e Tecnologia (FCT-Portugal).

Notes

The authors declare no competing financial interest.

■ ACKNOWLEDGMENTS

We thank Sergio Sánchez-Herrero for his help in handling the ITC equipment

DOI: 10.1021/acs.jafc.7b01600
J. Agric. Food Chem. XXXX, XXX, XXX−XXX

REFERENCES

(1) Monagas, M.; Gómez-Cordovés, C.; Bartolomé, B.; Laureano, O.; Ricardo Da Silva, J. M. Monomeric, oligomeric, and polymeric flavan-3-ol composition of wines and grapes from *Vitis vinifera* L. cv. Graciano, Tempranillo, and Cabernet Sauvignon. *J. Agric. Food Chem.* **2003**, *51*, 6475−6481.

(2) Ferrer-Gallego, R.; Quijada-Morín, N.; Brás, N. F.; Gomes, P.; de Freitas, V.; Rivas-Gonzalo, J. C.; Escribano-Bailón, M. T. Characterization of sensory properties of flavanols—a molecular dynamic approach. *Chem. Senses* **2015**, *40*, 381−390.

(3) Hufnagel, J. C.; Hofmann, T. Quantitative reconstruction of the nonvolatile sensometabolome of a red wine. *J. Agric. Food Chem.* **2008**, *56*, 9190−9199.

(4) Hufnagel, J. C.; Hofmann, T. Orosensory-directed identification of astringent mouthfeel and bitter-tasting compounds in red wine. *J. Agric. Food Chem.* **2008**, *56*, 1376−1386.

(5) Wollmann, N.; Hofmann, T. Compositional and sensory characterization of red wine polymers. *J. Agric. Food Chem.* **2013**, *61*, 2045−2061.

(6) Frank, S.; Wollmann, N.; Schieberle, P.; Hofmann, T. Reconstitution of the flavor signature of Dornfelder red wine on the basis of the natural concentrations of its key aroma and taste compounds. *J. Agric. Food Chem.* **2011**, *59*, 8866−8874.

(7) ASTM. *Standard Definitions of Terms Relating to Sensory Evaluation of Materials and Products*; American Society for Testing and Materials: Philadelphia, PA, USA, 2004.

(8) Ferrer-Gallego, R.; Hernández-Hierro, J. M.; Rivas-Gonzalo, J. C.; Escribano-Bailón, M. T. Sensory evaluation of bitterness and astringency sub-qualities of wine phenolic compounds: synergistic effect and modulation by aromas. *Food Res. Int.* **2014**, *62*, 1100−1107.

(9) Ma, W.; Guo, A.; Zhang, Y.; Wang, H.; Liu, Y.; Li, H. A review on astringency and bitterness perception of tannins in wine. *Trends Food Sci. Technol.* **2014**, *40*, 6−19.

(10) Gibbins, H. L.; Carpenter, G. H. Alternative mechanisms of astringency − what is the role of saliva? *J. Texture Stud.* **2013**, *44*, 364−375.

(11) Baxter, N. J.; Lilley, T. H.; Haslam, E.; Williamson, M. P. Multiple interactions between polyphenols and a salivary proline-rich protein repeat result in complexation and precipitation. *Biochemistry* **1997**, *36*, 5566−5577.

(12) Soares, S.; Mateus, N.; de Freitas, V. Interaction of different classes of salivary proteins with food tannins. *Food Res. Int.* **2012**, *49*, 807−813.

(13) Schwarz, B.; Hofmann, T. Is there a direct relationship between oral astringency and human salivary protein binding? *Eur. Food Res. Technol.* **2008**, *227*, 1693−1698.

(14) Messana, I.; Inzitari, R.; Fanali, C.; Cabras, T.; Castagnola, M. Facts and artifacts in proteomics of body fluids. What proteomics of saliva is telling us? *J. Sep. Sci.* **2008**, *31*, 1948−1963.

(15) Castagnola, M.; Cabras, T.; Vitali, A.; Sanna, M. T.; Messana, I. Biotechnological implications of the salivary proteome. *Trends Biotechnol.* **2011**, *29*, 409−418.

(16) Canon, F.; Ployon, S.; Mazauric, J. P.; Sarni-Manchado, P.; Réfrégiers, M.; Giuliani, A.; Cheynier, V. Binding site of different tannins on a human salivary proline-rich protein evidenced by dissociative photoionization tandem mass spectrometry. *Tetrahedron* **2015**, *71*, 3039−3044.

(17) de Freitas, V.; Mateus, N. Protein/polyphenol interactions: past and present contributions. Mechanisms of astringency perception. *Curr. Org. Chem.* **2012**, *16*, 724−746.

(18) Poncet-Legrand, C.; Gautier, C.; Cheynier, V.; Imberty, A. Interactions between flavan-3-ols and poly(L-proline) studied by isothermal titration calorimetry: effect of the tannin structure. *J. Agric. Food Chem.* **2007**, *55*, 9235−9240.

(19) Papadopoulou, A.; Frazier, R. A. Characterization of protein-polyphenol interactions. *Trends Food Sci. Technol.* **2004**, *15*, 186−190.

(20) Soares, S.; Mateus, N.; De Freitas, V. Interaction of different polyphenols with bovine serum albumin (BSA) and human salivary α-amylase (HSA) by fluorescence quenching. *J. Agric. Food Chem.* **2007**, *55*, 6726−6735.

(21) Brandão, E.; Santos Silva, M.; García-Estévez, I.; Mateus, N.; de Freitas, V.; Soares, S. Molecular study of mucin-procyanidin interaction by fluorescence quenching and saturation transfer difference (STD)-NMR. *Food Chem.* **2017**, *228*, 427−434.

(22) Cala, O.; Pinaud, N.; Simon, C.; Fouquet, E.; Laguerre, M.; Dufourc, E. J.; Pianet, I. NMR and molecular modeling of wine tannins binding to saliva proteins: revisiting astringency from molecular and colloidal prospects. *FASEB J.* **2010**, *24*, 4281−4290.

(23) Watrelot, A. A.; Renard, C. M. G. C.; Le Bourvellec, C. Comparison of microcalorimetry and haze formation to quantify the association of B-type procyanidins to poly-l-proline and bovine serum albumin. *LWT−Food Sci. Technol.* **2015**, *63*, 376−382.

(24) Pascal, C.; Poncet-Legrand, C.; Imberty, A.; Gautier, C.; Sarni-Manchado, P.; Cheynier, V.; Vernhet, A. Interactions between a non glycosylated human proline-rich protein and flavan-3-ols are affected by protein concentration and polyphenol/protein ratio. *J. Agric. Food Chem.* **2007**, *55*, 4895−4901.

(25) Papadopoulou, A.; Green, R. J.; Frazier, R. A. Interaction of flavonoids with bovine serum albumin: a fluorescence quenching study. *J. Agric. Food Chem.* **2005**, *53*, 158−163.

(26) Canon, F.; Paté, F.; Cheynier, V.; Sarni-Manchado, P.; Giuliani, A.; Pérez, J.; Durand, D.; Li, J.; Cabane, B. Aggregation of the salivary proline-rich protein IB5 in the presence of the tannin EgCG. *Langmuir* **2013**, *29*, 1926−1937.

(27) Dawes, C. Circadian rhythms in human salivary flow rate and composition. *J. Physiol.* **1972**, *220*, 529−545.

(28) Messana, I.; Cabras, T.; Inzitari, R.; Lupi, A.; Zuppi, C.; Olmi, C.; Fadda, M. B.; Cordaro, M.; Giardina, B.; Castagnola, M. Characterization of the human salivary basic proline-rich protein complex by a proteomic approach. *J. Proteome Res.* **2004**, *3*, 792−800.

(29) Soares, S.; Vitorino, R.; Osório, H.; Fernandes, A.; Venâncio, A.; Mateus, N.; Amado, F.; De Freitas, V. Reactivity of human salivary proteins families toward food polyphenols. *J. Agric. Food Chem.* **2011**, *59*, 5535−5547.

(30) Link, A. J.; Eng, J.; Schieltz, D. M.; Carmack, E.; Mize, G. J.; Morris, D. R.; Garvik, B. M.; Yates, J. R. Direct analysis of protein complexes using mass spectrometry. *Nat. Biotechnol.* **1999**, *17*, 676−682.

(31) Quijada-Morín, N.; Crespo-Expósito, C.; Rivas-Gonzalo, J. C.; García-Estévez, I.; Escribano-Bailón, M. T. Effect of the addition of flavan-3-ols on the HPLC-DAD salivary-protein profile. *Food Chem.* **2016**, *207*, 272−278.

(32) Inzitari, R.; Cabras, T.; Onnis, G.; Olmi, C.; Mastinu, A.; Sanna, M. T.; Pellegrini, M. G.; Castagnola, M.; Messana, I. Different isoforms and post-translational modifications of human salivary acidic proline-rich proteins. *Proteomics* **2005**, *5*, 805−815.

(33) Cabras, T.; Melis, M.; Castagnola, M.; Padiglia, A.; Tepper, B. J.; Messana, I.; Barbarossa, I. T. Responsiveness to 6-n-propylthiouracil (PROP) is associated with salivary levels of two specific basic proline-rich proteins in humans. *PLoS One* **2012**, *7*, e30962.

(34) Gururaja, T. L.; Levine, M. J. Solid-phase synthesis and characterization of human salivary statherin: a tyrosine-rich phosphoprotein inhibitor of calcium phosphate precipitation. *Pept. Res.* **1996**, *9*, 283−289.

(35) Halgand, F.; Zabrouskov, V.; Bassilian, S.; Souda, P.; Loo, J. A.; Faull, K. F.; Wong, D. T.; Whitelegge, J. P. Defining intact protein primary structures from saliva: a step toward the human proteome project. *Anal. Chem.* **2012**, *84*, 4383−4395.

(36) Vitorino, R.; Lobo, M. J. C.; Ferrer-Correira, A. J.; Dubin, J. R.; Tomer, K. B.; Domingues, P. M.; Amado, F. M. L. Identification of human whole saliva protein components using proteomics. *Proteomics* **2004**, *4*, 1109−1115.

(37) Frisch, M. J.; Trucks, H. B.; Schlegel, Scuseria, G. E.; Robb, M. A.; Cheeseman, J. R.; Scalmani, G.; Barone, V.; Mennucci, B.; Petersson, G. A.; Nakatsuji, H.; Caricato, M.; Li, X.; Hratchian, H. P.; Izmaylov, A. F.; Bloino, J.; Zheng, G.; Sonnenberg, J. L.; Hada, M.; Ehara, M.; Toyota, K.; Fukuda, R.; Hasegawa, J.; Ishida, M.; Nakajima,

DOI: 10.1021/acs.jafc.7b01600
J. Agric. Food Chem. XXXX, XXX, XXX−XXX

T.; Honda, Y.; Kitao, O.; Nakai, H.; Vreven, T.; Montgomery, Jr., J. A.; Peralta, J. E.; Ogliaro, F.; Bearpark, M.; Heyd, J. J.; Brothers, E.; Kudin, K. N.; Staroverov, V. N.; Kobayashi, R.; Normand, J.; Raghavachari, K.; Rendell, A.; Burant, J. C.; Iyengar, S. S.; Tomasi, J.; Cossi, M.; Rega, N.; Millam, N. J.; Klene, M.; Knox, J. E.; Cross, J. B.; Bakken, V.; Adamo, C.; Jaramillo, J.; Gomperts, R.; Stratmann, R. E.; Yazyev, O.; Austin, A. J.; Cammi, R.; Pomelli, C.; Ochterski, J. W.; Martin, R. L.; Morokuma, K.; Zakrzewski, V. G.; Voth, G. A.; Salvador, P.; Dannenberg, J. J.; Dapprich, S.; Daniels, A. D.; Farkas, Ö.; Foresman, J. B.; Ortiz, J. V.; Cioslowski, J.; Fox, D. J. *Gaussian 09*; Gaussian, Inc.: Wallingford, CT, USA, 2009; pp 2−3.

(38) Bayly, C. C. I.; Cieplak, P.; Cornell, W. D.; Kollman, P. a. A well-behaved electrostatic potential based method using charge restraints for deriving atomic charges: the RESP model. *J. Phys. Chem.* **1993**, *97*, 10269−10280.

(39) Wang, J.; Wolf, R. M.; Caldwell, J. W.; Kollman, P. A.; Case, D. A. Development and testing of a general amber force field. *J. Comput. Chem.* **2004**, *25*, 1157−1174.

(40) Hornak, V.; Abel, R.; Okur, A.; Strockbine, B.; Roitberg, A.; Simmerling, C. Comparison of multiple amber force fields and development of improved protein backbone parameters. *Proteins: Struct., Funct., Genet.* **2006**, *65*, 712−725.

(41) Izaguirre, J. A.; Catarello, D. P.; Wozniak, J. M.; Skeel, R. D. Langevin stabilization of molecular dynamics. *J. Chem. Phys.* **2001**, *114*, 2090−2098.

(42) Ryckaert, J. P.; Ciccotti, G.; Berendsen, H. J. C. Numerical integration of the cartesian equations of motion of a system with constraints: molecular dynamics of n-alkanes. *J. Comput. Phys.* **1977**, *23*, 327−341.

(43) Essmann, U.; Perera, L.; Berkowitz, M. L.; Darden, T.; Lee, H.; Pedersen, L. G. A smooth particle mesh Ewald method. *J. Chem. Phys.* **1995**, *103*, 8577−8593.

(44) Case, D. A.; Darden, T. A.; Cheatham, T. E.; Simmerling, C. L.; Wang, J.; Duke, R. E.; Luo, R.; Walker, R. C.; Zhang, W.; Merz, K. M.; Roberts, B.; Hayik, S.; Roitberg, A.; Seabra, G.; Swails, J.; Goetz, A. W.; Kolossváry, I.; Wong, K. F.; Paesani, F.; Vanicek, J.; Wolf, R. M.; Liu, J.; Wu, X.; Brozell, S. R.; Steinbrecher, T.; Gohlke, H.; Cai, Q.; Ye, X.; Wang, J.; Hsieh, M. J.; Cui, G.; Roe, D. R.; Mathews, D. H.; Seetin, M. G.; Salomon-Ferrer, R.; Sagui, C.; Babin, V.; Luchko, T.; Gusarov, S.; Kovalenko, A.; Kollman, P. A. *AMBER 12*; University of California: San Francisco, CA, USA, 2012.

(45) Humphrey, W.; Dalke, A.; Schulten, K. VMD: visual molecular dynamics. *J. Mol. Graphics* **1996**, *14*, 33−38.

(46) Velazquez-Campoy, A.; Ohtaka, H.; Nezami, A.; Muzammil, S.; Freire, E. Isothermal titration calorimetry. *Curr. Protoc. Cell Biol.* **2004**, 17.8.1−17.8.24.

(47) Mariana, F.; Buchholz, F.; Harms, H.; Yong, Z.; Yao, J.; Maskow, T. Isothermal titration calorimetry − a new method for the quantification of microbial degradation of trace pollutants. *J. Microbiol. Methods* **2010**, *82*, 42−48.

(48) Frazier, R. A.; Papadopoulou, A.; Green, R. J. Isothermal titration calorimetry study of epicatechin binding to serum albumin. *J. Pharm. Biomed. Anal.* **2006**, *41*, 1602−1605.

(49) Frazier, R. A.; Papadopoulou, A.; Mueller-Harvey, I.; Kissoon, D.; Green, R. J. Probing protein-tannin interactions by isothermal titration microcalorimetry. *J. Agric. Food Chem.* **2003**, *51*, 5189−5195.

(50) Prigent, S. V. E.; Voragen, a G. J.; van Koningsveld, G. a; Baron, A.; Renard, C. M. G. C.; Gruppen, H. Interactions between globular proteins and procyanidins of different degrees of polymerization. *J. Dairy Sci.* **2009**, *92*, 5843−5853.

(51) Simon, C.; Barathieu, K.; Laguerre, M.; Schmitter, J. M.; Fouquet, E.; Pianet, I.; Dufourc, E. J. Three-dimensional structure and dynamics of wine tannin-saliva protein complexes. A multitechnique approach. *Biochemistry* **2003**, *42*, 10385−10395.

(52) De Freitas, V.; Carvalho, E.; Mateus, N. Study of carbohydrate influence on protein-tannin aggregation by nephelometry. *Food Chem.* **2003**, *81*, 503−509.

(53) Kilmister, R. L.; Faulkner, P.; Downey, M. O.; Darby, S. J.; Falconer, R. J. The complexity of condensed tannin binding to bovine serum albumin − an isothermal titration calorimetry study. *Food Chem.* **2016**, *190*, 173−178.

(54) Kallithraka, S.; Bakker, J. Evaluation of bitterness and astringency of (+)-catechin and (−)-epicatechin in red wine and in model solution. *J. Sens. Stud.* **1997**, *12*, 25−37.

(55) Thorngate, J. H.; Noble, A. C. Sensory evaluation of bitterness and astringency of 3R(−)-epicatechin and 3S(+)-catechin. *J. Sci. Food Agric.* **1995**, *67*, 531−535.

(56) Allen, M. P. Introduction to molecular dynamics simulation. In *Computational Soft Matter: From Synthetic Polymers to Proteins*; Gustav-Stresemann-Institute: Bonn, Germany, 2004; Vol. 23, pp 1−28.

(57) Ferrer-Gallego, R.; Hernández-Hierro, J. M.; Brás, N. F.; Vale, N.; Gomes, P.; Mateus, N.; de Freitas, V.; Heredia, F. J.; Escribano-Bailón, M. T. Interaction between wine phenolic acids and salivary proteins by saturation-transfer difference nuclear magnetic resonance spectroscopy (STD-NMR) and molecular dynamics simulations. *J. Agric. Food Chem.* **2017**, DOI: 10.1021/acs.jafc.6b05414.

(58) Quijada-Morín, N.; Regueiro, J.; Simal-Gándara, J.; Tomás, E.; Rivas-Gonzalo, J. C.; Escribano-Bailón, M. T. Relationship between the sensory-determined astringency and the flavanolic composition of red wines. *J. Agric. Food Chem.* **2012**, *60*, 12355−12361.

DOI: 10.1021/acs.jafc.7b01600
J. Agric. Food Chem. XXXX, XXX, XXX−XXX